Haile *et al. EURASIP Journal on Wireless Communications and Networking* (2015) 2015:78
DOI 10.1186/s13638-015-0279-4

EURASIP Journal on Wireless Communications and Networking
a SpringerOpen Journal

RESEARCH Open Access

Coordinated multi-point transmission for relaxation of self-backhauling bottlenecks in heterogeneous networks

Beneyam B. Haile*, Edward Mutafungwa and Jyri Hämäläinen

Abstract

The heterogeneous deployment of high-power macro cells and low-power nodes (LPNs) is now widely acknowledged as an essential requirement towards meeting the continued demand for mobile data capacity. The selection of the optimum backhaul solution for the LPNs obliges operators to consider not only the capacity of the backhaul but also other key factors so as to fully leverage the benefits provided by LPNs: the cost of the backhauling may limit the density of LPN deployments and the backhaul configuration requirements impact on the flexibility of LPN deployment. To that end, self-backhauling of LPNs via the existing macro radio access network (RAN) provides an attractive solution, particularly for deployment scenarios that are very cost-sensitive and/or require high flexibility. However, use of self-backhauling usually makes backhaul as a bottleneck due to the a) limited bandwidth allocated for legacy macro RAN, b) the need to share resources with macro user equipment (UE), and c) the high-intercell interference particularly in the macro cell edge. In this paper, we provide an overview of self-backhauled LPNs and investigate possible performance enhancements through the use of coordinated multi-point (CoMP) transmission to relax the downlink backhaul capacity bottleneck for self-backhauled LPNs. To that end, we carry out analytical studies for a practical limited-feedback CoMP technique and numerically verify the derived capacity outage expressions. Furthermore, we implement a simulation study for an exemplary heterogeneous network deployment in a realistic radio propagation environment. The results of the studies demonstrate that significant spectral efficiency and throughput gains for the LPN backhaul are achievable through the use of selected CoMP technique under realizable feedback overhead, even under feedback bit error. The achieved relaxation in the backhaul bottleneck is observed providing improved performance for the UEs served by the LPNs. Furthermore, more resources will be available for macro UEs leading to overall performance gains compared to the case without CoMP.

Keywords: Coordinated multi-point transmission; LTE-advanced; Low-power nodes; Small cells; Relays; Backhaul

1 Introduction

1.1 Background

Mobile network operators face the challenge of upgrading their networks to handle increased mobile data traffic from certain locations (hot spots or hot zones) and meet user expectations for cellular coverage in every location [1]. While the approach of scaling network capacity by increasing available spectrum and improving spectral efficiency provides considerable scaling in network capacity, even more substantial growth is possible by reusing spectrum through network densification [1-3]. The commonly considered network densification approach is through the heterogeneous deployment of low-power nodes (typically 10 W or lower) to complement traditional high-power (20 W or higher) macro sites [1-5]. The term *low-power node* (LPN) is adopted in this paper to draw a distinction between the added complementary LPNs and the legacy macro sites in a heterogeneous network (HetNet) environment.

A diverse range of LPNs exist depending on various practical considerations. These include drivers for LPN deployment (need to improve coverage, capacity, or both) and attributes of the coverage area, such as area size and

*Correspondence: beneyam.haile@aalto.fi
School of Electrical Engineering, Aalto University, P.O. Box 13000, FI-00076 Aalto, Espoo, Finland

location (indoor or outdoor). The LPNs include small cells and extensions to macro cells, such as relays, remote radio heads (RRHs), and distributed antenna systems (DAS). Small cells is itself an umbrella term for compact base stations deployed to enhance coverage and capacity in homes, enterprise environments, under-served areas, and indoor or outdoor public spaces [2]. Operator deployed small cells include metrocells, microcells, picocells, and open access femtocells. On the other hand, indoor closed-access femtocells are deployed and operated by end users in their place of residence, analogous to traditional WiFi access points.

1.2 LPN backhauling options

The reduced size and weight of LPNs allows them to be deployed rapidly, cost-effectively, and on a relatively wider range of locations compared to traditional macro sites [6]. Typical LPN deployment locations include street furniture (e.g., lamp posts or utility poles), on the side of buildings below rooftop level, on vehicle rooftops, and so on. However, while benefiting from this added deployment flexibility, the operator has still to carefully consider LPN site selection to ensure accessibility for LPN site maintenance while simultaneously securing the LPN site assets from malicious intruders. Furthermore, reliable operation of LPNs requires assured access to uninterrupted power sources and high-capacity backhaul links [5-8].

In this paper, we focus on the LPN backhauling challenge. A number of LPN backhauling solutions are possible depending on the LPN deployment scenario [6,7]. Indoor-deployed LPNs (e.g., enterprise femtos) can be backhauled using existing in-building wireline infrastructure, such as copper twisted-pair digital subscriber lines (DSL), fiber, and coaxial cables (for cable television). Outdoor-deployed LPNs in most cases do not have access to legacy cabling and the cost of targeted roll-out of cables to each LPN would be prohibitive [6]. Therefore, wireless backhauling solutions, such as microwave radio links (<7 GHz, 6 to 50 GHz), millimeter wave and E-band radio links (57 to 66 GHz, 71 to 95 GHz), and free-space optics and satellite, are usually considered for outdoor LPNs [6-8]. The differentiating attributes for the different wireless backhaul solutions include the following:

- *Deployment topology:* Configuration between LPNs and backhaul hub point. Common configurations are point-to-point (P2P), point-to-multipoint (P2MP), tree, and mesh topologies.
- *Line-of-sight (LOS) requirements:* The LOS requirements vary from demand for strict LOS to near LOS (nLOS) and non-LOS (NLOS) links.
- *Operating spectrum band:* Differs depending on spectrum licensing arrangements (licensed or unlicensed bands). Differences may also be in spectrum allocation between LPN backhaul and access links, whereby utilized spectrum bands are either overlapping (inband) or orthogonal (outband) between the access and backhaul links.
- *Capacity:* Typical capacity (bits per second) available over the backhaul link.

These aforementioned attributes strongly influence the selection of wireless backhaul solution for a particular deployment scenario. Typically, LPN operators have to consider the trade-offs among factors, such as required performance, operating costs, and feasibility or ease of deployment [6-8]. In this study, we focus on wireless backhauling solutions for LPNs that are strongly constrained by cost and demand high flexibility in terms of deployment. The highly flexible backhaul is desirable since it usually implies rapid unplanned deployment of the LPN network expansion with no intervention from the operator. Example scenarios that demand such cost-sensitive and highly flexible backhauling include the following: densely populated areas [9]; semi-permanent networks (e.g., for open air festivals) [9]; and spontaneous or rapid network deployment scenarios (e.g., public safety communications) [9-11].

1.3 Self-backhauled LPN

1.3.1 Description and benefits

Self-backhauling of LPNs via the existing macro radio access network (RAN) is an attractive backhauling solution for certain LPN deployment scenarios. In Figure 1, we provide a simple illustration to describe the difference between conventional fixed-wireless backhauling and self-backhauling for LPNs. Conventional wireless backhauling for LPNs relies on dedicated P2P or P2MP fixed-wireless technologies (e.g., millimeter wave radios) with stringent LOS requirements between the LPN and the wireless hub which may be collocated with a macro site (see Figure 1a). The LOS requirements for fixed-wireless backhauling links can be relaxed through use of multi-hop mesh or tree topologies to route the fixed-wireless links around shadowing objects (e.g., tall buildings) [6].

By contrast, in Figure 1b, self-backhauling is provided via the macro RAN for LPNs deployed within the coverage area of a particular macrocell, with the macrocell resources being shared by other LPNs and/or macro user equipment (UE) located within the same coverage area.

The LPN self-backhauling approach provides a number of benefits compared to conventional fixed-wireless backhauling. These include the following:

- Cost savings by leveraging existing macrocell site infrastructure (e.g., radio towers, standby batteries) for small cell backhauling;

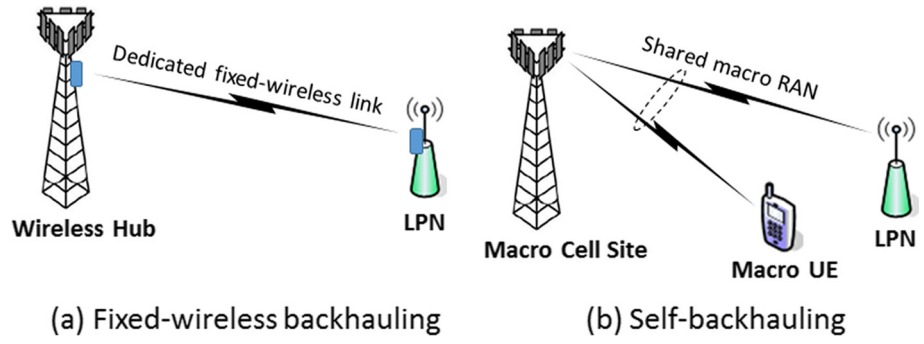

Figure 1 Backhauling of LPN using (a) fixed-wireless links and (b) self-backhauling via macro RAN.

- Further cost saving through possible reuse of spectrum bands licensed to the macro network operator and resource sharing over a number of LPNs (as opposed to having dedicated backhaul links to each LPN);
- Wireless backhaul in NLOS conditions using legacy cellular spectrum bands (typically below 3.5 GHz) and emerging lightly licensed bands (e.g., TV white space) with good RF propagation properties; and
- Possible joint radio resource management (RRM) implementation for the LPN backhaul and access links [12].

These self-backhauling benefits have motivated the development of the relaying concept introduced in Long Term Evolution (LTE)-Advanced. Relaying is a LPN solution, whereby, compact relay nodes (RNs) are wirelessly self-backhauled via a standardized LTE relay link (Un interface) towards a macro donor eNode B (DeNB) [13]. The relay access links towards the UEs are then based on the conventional LTE Uu air interface.

However, the self-backhauling approach can be extended to include all types of LPNs (beyond relays). This is based on the possible flexibility in selection of radio access technologies (RATs) and operating spectrum band strategies between the LPN backhaul (in this case, macro access) and LPN access links. The viability of this approach has been recognized in both research community and industry. For instance, Qualcomm proposes the use of so-called 'Velcro relays', whereby, macro LTE provides backhauling for evolved 3G small cells (HSPA+/EV-DO) in places with low-penetration user LTE [14]. The architectural arrangement of having a 'hub base station' as a concentration point of self-backhauled small cells has also been investigated in a recently completed project (FP7 BuNGee [15]). Notably, there have also been recent standardization activities for specification of the use of WiMAX air interface for small cell backhauling (IEEE 802.16r [16]).

1.3.2 Backhaul capacity bottleneck

The self-backhauling of Figure 1b, with use of macro resources in the backhaul, is key factor while utilizing the benefits of cost-effectiveness and flexibility in LPN deployment. However, the reuse of the macro resources usually results in a backhaul capacity bottleneck, whereby the aggregate served capacity of LPN access exceeds the achievable wireless backhaul capacity. This self-backhauling capacity bottleneck will consequently limit peak achievable throughputs for the UE served by the LPN.

Self-backhaul link capacity enhancements have been considered previously particularly for relay deployments. Proposals include strategies that optimize DeNB selection and placement of RN to provide signal-to-interference-and-noise ratio (SINR) gain for the relay backhaul link, particularly at the cell edge [17-19]. Unfortunately, these SINR gains may be difficult to achieve in practical deployments, due to the challenge of site acquisition that often limits the available set of good candidate locations. Additional capacity enhancements of self-backhauled links are being considered by increasing spectral-efficiency through higher-order modulations (256 QAM or higher) and complex multiple-input and multiple-output (MIMO) configurations [16]. However, these spectral-efficiency enhancements require proximity to macrocell center (to guarantee high SINR for the backhaul link) and rich scattering environments (for backhaul channel capacity to scale linearly with number of antennas) in order to achieve their full potential.

Other self-backhauling capacity enhancement approaches considered include the backhaul resource allocation among a group of small cells based on the relative load (number of served UEs) of each small cell [20]. The capacity gains (scheduling gains) from this approach are dependent on the differential loading among the scheduled small cells and are still constrained by the overall level of resources allocated for small cell backhaul. Additional joint optimization of resource distribution for

self-backhaul and small cell access has been considered for operator-shared small cells, with additional requirements of cooperative signaling information exchange across different operators [12].

1.4 Paper contribution and structure

In this paper, we propose an approach for relaxing the self-backhauled LPN capacity bottleneck by providing backhaul link SINR gains at the cell edge through the use of coordinated multi-point (CoMP) joint transmission (JT) in a frequency-division duplexing (FDD) downlink system. CoMP JT is an LTE-Advanced enhancement proposed to improve the achievable cell edge SINR through combination of transmissions from two or more neighboring cells that simultaneously serve a selected UE [21,22]. The CoMP approach is feasible since the self-backhauled LPN appears like a regular UE over the backhaul link to the serving macrocell.

We present an analytical expression of capacity outage probability for a practical limited-feedback CoMP technique considering Rician fading channel towards the donor cell and Rayleigh fading channels towards the rest of the cells in CoMP set. The Rician fading channel towards the donor cell is based on the assumption that LPNs have LOS connection from their donor cells, which is mostly the intended scenario in practice. Previously, outage capacity analysis was carried out for CoMP systems in [23] while authors in [24] provide analysis on optimal power allocation. Distinction of our work is that analyses in both works consider Rayleigh fading channels for all base station transmissions. Furthermore, [23] presents results for CoMP methods exploiting long-term channel feedback whereas [24] provides results for CoMP methods utilizing perfect channel feedback. We provide outage capacity analysis for 3rd Generation Partnership Project (3GPP) compliant CoMP method that exploits quantized short-term phase feedback. We also present an exemplary simulation study which considers LTE-Advanced relays as the LPNs served by macrocells. In that simulation study, use of limited-feedback CoMP technique to relax relay bottlenecks is considered for a selected realistic deployment scenario. Deterministic dominant path model is used for propagation computation. We provide insight on combining the CoMP and resource scheduling for improved performance. Furthermore, we provide additional insights on possible performance degradations due to different levels of feedback errors.

Analytical results demonstrate that the CoMP method can significantly increase targeted capacity for a given outage probability; and even with low feedback overhead, the limited-feedback method performs close to the ideal maximum ratio transmission that requires full channel state information (CSI) at the transmitter. From simulation results, we observe that the CoMP method provides considerable backhaul throughput gain and narrows down the capacity gap between backhaul and access. Furthermore, we demonstrate the achieved gain either directly improving relay UE throughput or throughput of all UEs (including macro UEs) by impacting applied scheduling method. The CoMP gain results in improved throughput fairness among the whole UE population. Moreover, these benefits of CoMP at relay backhaul is sustained under feedback error although considerable reduction is observed for large ($\geq 10\%$) bit error probability.

The rest of the paper is structured as follows. In Section 2, we present the system model, the limited-feedback CoMP method, and an overview of the possible resource allocation strategies. In Section 3, we derive expression for the capacity outage probability and provide respective performance evaluation. In Section 4, we present the simulation study on CoMP applied at the backhaul of LTE-Advanced relays highlighting throughput results and observations. Finally, conclusions and suggestions for future work are given in Section 5.

2 System model, CoMP scheme, and resource allocation

2.1 System model

Figure 2 depicts a HetNet deployment scenario where macrocell resources are employed to self-backhaul LPN and to enhance coverage and/or capacity. In the non-CoMP case, the LPN backhaul is provided by the serving macrocell only, while the signals of the adjacent macrocells appear as interference. Moreover, in the CoMP case, the self-backhauling of the small cell is provided jointly by all the coordinating macrocells.

We consider flat and block-fading channel model. Thus, channel gains remain constant during each frame/block of transmitted symbols and gains from different blocks are independent. We assume Rayleigh fading channel for all links between macro base stations and the LPNs exception being the donor cell which we assume to have a LOS connection to the LPN with the channel experiencing Rician fading. Thus, channel gains $h_j = \sqrt{\xi_j}e^{j\phi_i}, j \neq 1$ are Rayleigh random variables where the channel power ξ_i follows exponential distribution with mean $\bar{\xi}_j = \mathbb{E}\{\xi_j\}$. On the other hand, donor cell channel gain $h_1 = \sqrt{\xi_1}e^{j\phi_1}$ is Rician random variable with mean channel power $\bar{\xi}_1 = \mathbb{E}\{\xi_1\}$ and Rician factor K. We note that the Rician model is most feasible for well-planned outdoor and above rooftop LPNs, but the model can also hold for other deployment scenarios with proper selection of K. We also assume that channels are non-identical (i.e., $\bar{\xi}_j \neq \bar{\xi}_i,\ i \neq j$) taking into account the distributed nature of LPN deployment and/or different main lobe directivity among antennas.

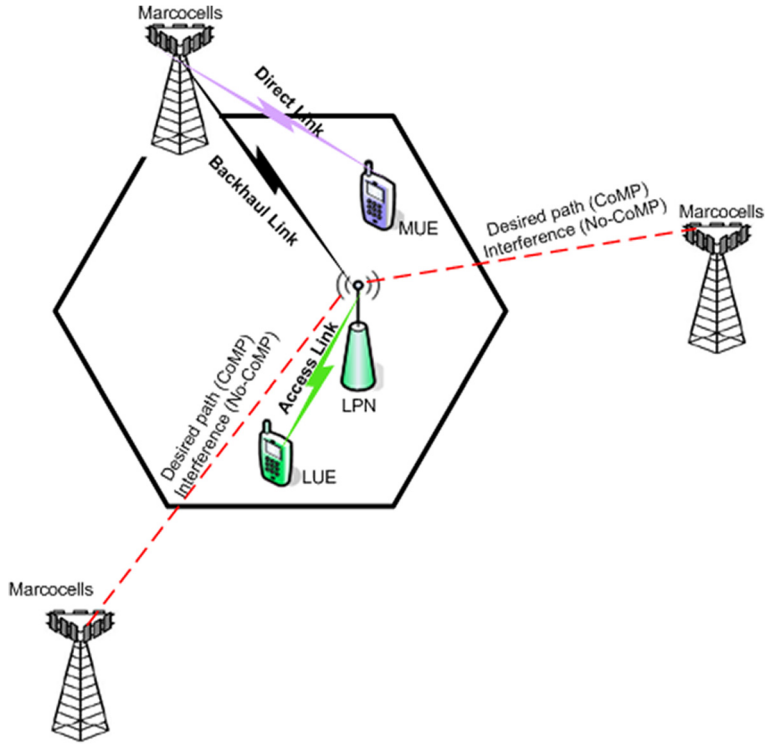

Figure 2 System illustration for considered HetNet. LUE refers to UE associated to LPN.

In the absence of coordination, the received signal in the self-backhauled LPN at a given arbitrary time instant is given by:

$$r = h_1 s_1 + \sum_{j \neq 1} h_j s_j + n, \tag{1}$$

where s_j is the transmitted information symbol from the jth macrocell such that $E[\,|s_j|^2] = P_t$, h_j is the channel from the jth macrocell, and n is zero-mean complex additive Gaussian noise with power P_N. Note that index 1 refers to the donor cell to which the LPN is associated.

When we consider coordination over the backhaul links, we apply JT from macrocells in a given CoMP set. The set comprises the donor cell and other selected macrocells based on the LPN average received signal power. We recall here that JT is one major CoMP subcategory defined in 3GPP, whereby, coordinating cells simultaneously serve a given CoMP node [22]. With JT CoMP, the received signal at the LPN becomes:

$$r = \sum_{j \in C} h_j \hat{w}_j s_1 + \sum_{j \notin C} h_j s_j + n, \tag{2}$$

where C denotes the CoMP set and $\hat{w}_j$ is selected precoding weight at the jth coordinating cell based on a given precoding method.

We consider a quantized feedback method that can be realized in FDD system due to limited feedback capacity requirement. The LPN estimates channels and selects appropriate weights based on the estimated channels and a given code book known at the coordinating cells and the LPN. The LPN then sends feedback bits identifying selected weights to the coordinating macrocells using error-free and delay-free feedback channel so that the macrocells apply selected weights in transmission. We note here that erroneous feedback will be considered later in the paper (Section 4.3) to analyze its impact on achieved results. As the same symbol s_1 is transmitted from coordinating cells, we assume that the information symbol is available among macrocells in C. Here, the assumption is that macrocells admit an ideal backhaul although they are located in different geographical locations.

2.2 Quantized co-phasing CoMP scheme

There are various precoding methods for coordination among cells under JT category with different performance and implementation requirements [22,25-28]. The JT CoMP method we consider in this work is based on short-term quantized phase information and relative phase-shifting operation referred to as quantized co-phasing (QCP) [29-31].

In QCP CoMP method, the LPN considers the channel from donor macrocell h_1 as a reference channel and set

the corresponding weight $\hat{w}_1 = 1/\sqrt{b}$, where b is a parameter that determines transmit power of macrocells in C. It is set to 1 when we assume full transmission power from each cell whereas it is set to the number of macrocells in C when power is normalized. Then, for each of remaining cells in C, the LPN selects weights $\hat{w}_j$ based on:

$$\hat{w}_j = \arg_{w_n \in \mathbf{W}} \max |h_1 + h_j w_n|, \tag{3}$$

where the code book $\mathbf{W}_j$ is given as:

$$\mathbf{W}_j = \left\{ w_n = \frac{1}{\sqrt{b}} e^{j\varphi_n} : \varphi_n = \pi n / 2^{N_j - 1}, n = 0, \ldots, 2^{N_j} - 1 \right\}. \tag{4}$$

The code book $\mathbf{W}_j$ is known by the LPN and respective coordinating macrocells, and its size depends on value of N_j which is number of bits used to report selected codeword to the macrocell.

This QCP method is suboptimal while it can be implemented in FDD systems with realizable feedback capacity requirement. If $N = 2$ and only two cells coordinate, then the method resembles closed-loop transmit diversity that is applied in HSDPA and LTE [32,33].

2.3 Resource allocation

The co-deployment of macrocells providing umbrella coverage over LPN hot spots is the commonly considered two-tier heterogeneous network deployment approach [1-5]. The implementation of self-backhauling in these two-tier networks presents a number of strategic options for RAN resource allocation (time resources, frequency resources, etc.) across three layers, namely macro access, LPN backhaul, and LPN access (see Figure 3). The orthogonal resource allocation (see Figure 3a) eliminates cross-layer co-channel interference but is inefficient due to lack of resource reuse. On the other hand, full sharing (see Figure 3f) achieves the high resource utilization at the cost of excessive cross-layer interference.

The alternative for co-channel deployment of macro access with resources shared between either LPN access or backhaul (see Figure 3(b),(c)) provides a trade-off between interference reduction and resource reuse efficiency. However, the reuse of the macro resources in both cases results in a backhaul capacity bottleneck, whereby the aggregate served capacity of LPN access exceeds the achievable LPN backhaul capacity. This will consequently limit peak achievable throughputs for the UE served by the LPN. The backhaul capacity bottleneck

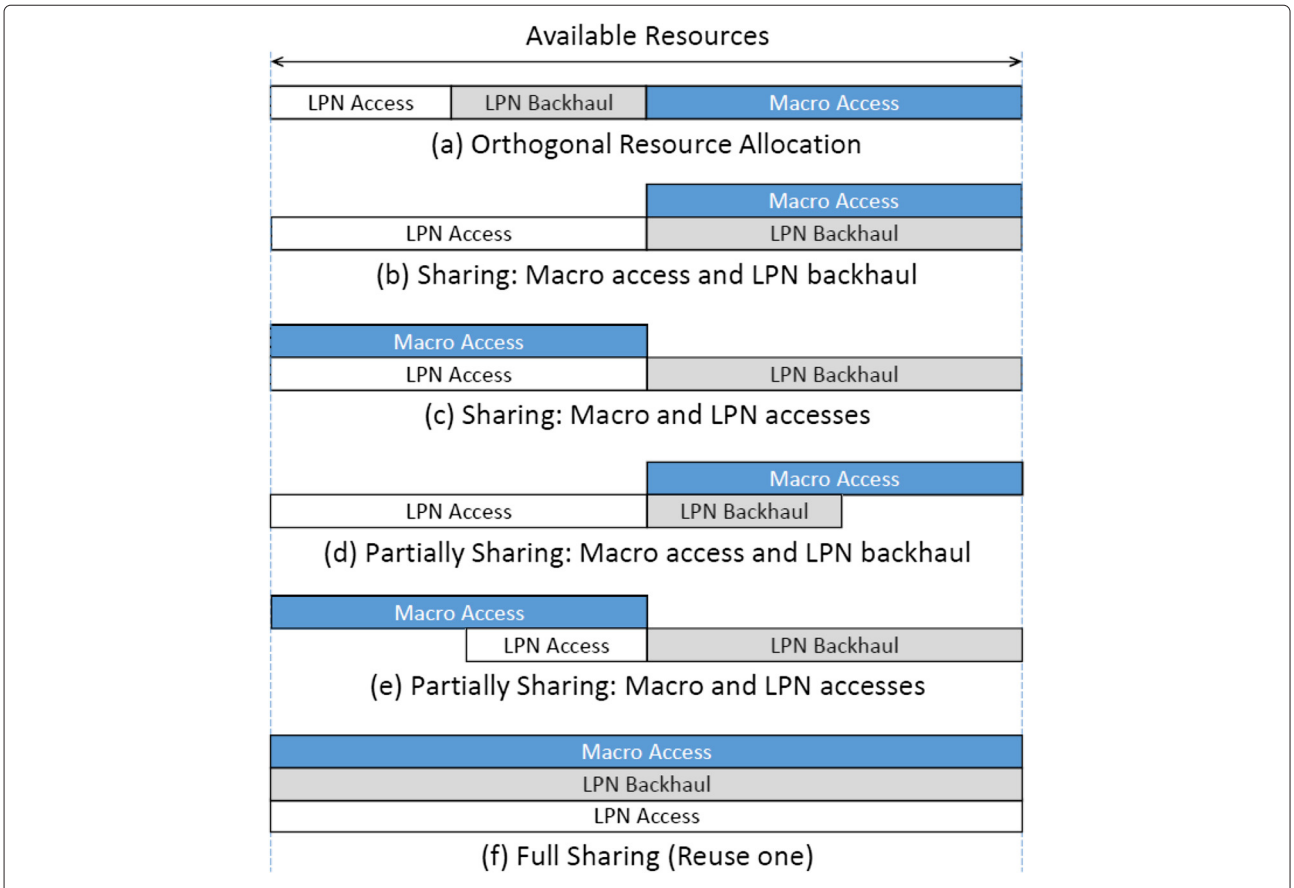

Figure 3 Possible resource allocation strategies in heterogeneous networks with self-backhauled LPNs.

is attributed to radio resource contention between LPN backhaul and existing macro UE (for resource allocation scheme of Figure 3(b)) or limits on RAN resource that can be exclusively dedicated for LPN backhauling (Figure 3(c)). Further backhaul capacity limitations occur due to inter-cell interference between adjacent macrocells which reduces SINR, particularly for self-backhauled LPNs deployed in the macrocell edge. Partial sharing of macro access resources (see Figure 3(d),(e)) may provide opportunities for reduced inter-cell interference but with the consequence of decreased resource utilization efficiency.

In this work, we assume that macro access share time resource with LPN access as shown in Figure 3(c) while frequency resource is fully reused in all layers. This provides best interference scenario for the backhaul link that it is not interfered by both the macro and the LPN accesses. This assumption is consistent with the resource-sharing strategy adopted in 3GPP for LTE-Advanced type I relays. However, we note here that even with these interference mitigation measures and relatively large resource allocation, the backhaul link could create a bottleneck as discussed in further detail later in Section 4.

3 Outage capacity analysis

In this section, we present analysis for the CoMP method performance gain in terms of outage capacity. For a required capacity $C_r = \log_2(1 + Z_r)$ in the backhaul, the outage probability is defined as:

$$P_o = P(Z < Z_r), \tag{5}$$

where Z is instantaneous SINR at the LPN and Z_r is the required SINR to meet the targeted capacity.

3.1 Outage probability analysis

In the absence of CoMP, all macrocell transmissions except transmission from donor cell are interfering the LPN backhaul link; hence the instantaneous SINR denoted by Z_{nc} attains the form:

$$Z_{nc} = \frac{\gamma_1}{\sum_{j\neq 1}\gamma_j + P_n}, \tag{6}$$

where received powers are $\gamma_j = P_t\xi_j$. We note here that γ_1 is power of Rician channel with mean value $\bar{\gamma}_1 = P_t\bar{\xi}_1$ and γ_j, $j \neq 1$ follows exponential distribution with mean $\bar{\gamma}_j = P_t\bar{\xi}_j$. If we assume network is interference limited, then Equation 6 becomes Rician/Rayleigh scenario, whereby the closed-form expression for outage probability is presented in [34]. Accordingly, we find that for non-CoMP case, an outage probability expression of the form:

$$P_o^{nc} = 1 - \sum_{j\neq 1} D_j \left[1 - \frac{\bar{\gamma}_j(K+1)Z_r}{\bar{\gamma}_1 + \bar{\gamma}_j(K+1)Z_r} * \exp\left(\frac{-K\bar{\gamma}_1}{\bar{\gamma}_1 + \bar{\gamma}_j(K+1)Z_r}\right)\right], \tag{7}$$

where $D_j = \prod_{i\neq j}\bar{\gamma}_j/\left(\bar{\gamma}_j - \bar{\gamma}_i\right)$.

When we apply QCP CoMP, some previously interfering links are now exploited to enhance the backhaul link; and the SINR denoted by Z_c takes the form:

$$Z_c = \frac{|\sum_{j\in C}\sqrt{\gamma_j}e^{j\phi_j}\hat{w}_j|^2}{\sum_{j\notin C}\gamma_j + P_n}. \tag{8}$$

Without loss of generality, we focus on the case where the number of macrocells in the CoMP set is limited to 3 although analysis for more than three macrocells is doable but long and impractical. In well-planned mobile network, strong signals are usually received only from two or three base stations while signals from other base stations are weaker. Let coordination takes place among donor cell and two other selected cells (indexed by 2 and 3) to serve the LPN. Then, utilizing weights $\hat{w}_j$ determined from Equation 3, we write the tight lower-bound outage probability P_o^c in the form:

$$P_o^c = P\left(\hat{Z}_c < Z_r\right), \tag{9}$$

where:

$$\hat{Z}_c = \frac{|\sqrt{\gamma_1} + \sqrt{\gamma_2}e^{j\theta_2} + \sqrt{\gamma_3}e^{j\theta_3}|^2}{b\sum_{j\notin C}\gamma_j}. \tag{10}$$

We note that $\theta_j = \phi_j - \phi_1 + \varphi_n$ is uniformly distributed on the range $\left(-\pi/2^{N_j}, \pi/2^{N_j}\right)$. As the channels are independent, we can write the outage probability in the form:

$$P_o^c = 1 - \int_0^\infty F_{\eta_2}(z/Z_r)f_{\eta_1}(z)dz, \tag{11}$$

where $F_{\eta_2}(\cdot)$ is the cumulative distribution function (CDF) of $\eta_2 = b\sum_{j\notin C}\gamma_j$ and $f_{\eta_1}(\cdot)$ is the probability distribution function (PDF) of $\eta_1 = |\sqrt{\gamma_1} + \sqrt{\gamma_2}e^{j\theta_2} + \sqrt{\gamma_3}e^{j\theta_3}|^2$. The CDF of η_2 is well-known that [35]:

$$F_{\eta_2}(z) = \sum_{j\notin C} D_j\left(1 - e^{\frac{-z}{b\bar{\gamma}_j}}\right), \tag{12}$$

where $D_j = \prod_{i\neq j, i\notin C}\bar{\gamma}_j/\left(\bar{\gamma}_j - \bar{\gamma}_i\right)$. We then substitute Equation 12 into Equation 11 and obtain:

$$P_o^c = 1 - \sum_{j\notin C} D_j\left(1 - \int_0^\infty e^{-\frac{z}{b\bar{\gamma}_j Z_r}}f_{\eta_1}(z)dz\right). \tag{13}$$

To solve the integral in Equation 13, we approximate PDF of η_1 using error corrected chi-squared distribution with 6

degrees of freedom (see Appendix A in [36]). The approximation is based on the fact that η_1 follows chi-squared distribution when $K = 0$, and full CSI is available at the coordinating macrocells. Thus:

$$f_{\eta_1}(z) = \frac{m^3 e^{-mz}}{2} \sum_{i=1}^{3} a_i z^{i+1}, \tag{14}$$

where $m = 3/\mathrm{E}[\eta_1]$, $a_3 = 2m^2\left(m^2\mathrm{E}\left[\eta_1^2\right]/48 - 0.25\right)$, $a_2 = -8a_3/m$, and $a_1 = -\mathrm{E}[\eta_1]\,a_2/2 + 1$. Let expand η_1 as:

$$\begin{aligned}\eta_1 = \gamma_1 + \gamma_2 + \gamma_3 + 2\sqrt{\gamma_1}\sqrt{\gamma_2}\cos\theta_2 + 2\sqrt{\gamma_1}\sqrt{\gamma_3}\cos\theta_3 \\ + 2\sqrt{\gamma_2}\sqrt{\gamma_3}\cos\theta_2\cos\theta_3 + 2\sqrt{\gamma_2}\sqrt{\gamma_3}\sin\theta_2\sin\theta_3,\end{aligned} \tag{15}$$

and from Equation 15 and its square, we compute first and second moments of η_1 based on expected values of γ_n^{δ} $(n = 1, 2, 3,\ \delta = 1/2, 1, 3/2)$, $\cos^{\iota}\theta_i$ and $\sin^{\iota}\theta_i$ $(i, \iota = 2, 3)$. Accordingly, we find:

$$\begin{aligned}\mathrm{E}[\eta_1] =& \bar{\gamma}_1 + \bar{\gamma}_2 + \bar{\gamma}_3 + \frac{\pi}{2}\sqrt{\frac{\bar{\gamma}_1}{K+1}}M(-1/2, 1; -K)* \\ & \left[\sqrt{\bar{\gamma}_2}C_2 + \sqrt{\bar{\gamma}_3}C_3\right] + \frac{\pi\sqrt{\bar{\gamma}_2\bar{\gamma}_3}C_2C_3}{2},\end{aligned} \tag{16}$$

where $M(a, b, z)$ is the confluent hypergeometric function defined in ([37], [13.2.1]), and $C_j = \mathrm{E}[\cos\theta_j] = \mathrm{sinc}(\pi/N_j)$. For simplicity, we do not present the attained expression for $\mathrm{E}[\eta_1^2]$ as it has a longer form. Finally, we substitute Equation 14 into Equation 13 and solve the integral to find an outage probability expression of the form:

$$\begin{aligned}P_o^c = 1 - \sum_{j\notin C} D_j \\ \times \left(1 - \frac{m^3}{2}\sum_{i=1}^{3} a_i(i+1)!\left(\frac{b\bar{\gamma}_j Z_r}{1 + mb\bar{\gamma}_j Z_r}\right)^{i+2}\right).\end{aligned} \tag{17}$$

3.2 Validation of outage capacity analysis

Figure 4 illustrates outage probability as a function of targeted capacity. Solid curves refer to analytical results and markers refer to numerical results. For benchmarking purposes, we also present numerical results for the ideal maximum ratio transmission that requires full CSI at coordinating cells, depicted with dashed and dash-dotted curves in Figure 4. All results are obtained for LPN1 shown in Figure 5 that depicts an irregular but realistic HetNet deployment scenario. The scenario will be explained further in Section 4, but for now, we note here that average channel powers computed based on a dominant path loss model. Furthermore, the Rician factor K is set to 3 dB; and the number of feedback bits N_1 and N_2 are both set to 3.

We can see from Figure 4 that the outage probability analysis and approximation presented in Subsection 3.1 are well validated. The QCP CoMP technique significantly improves the outage probability performance of the LPN relative to the non-CoMP case. For instance, 4.37- and

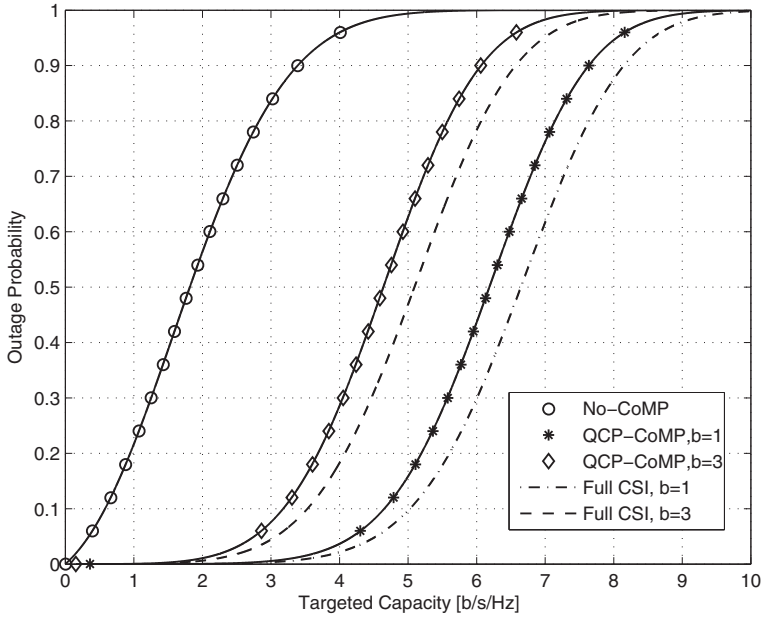

Figure 4 Outage probability as a function of required capacity. Solid curves refer to analytical results, markers refer to numerical results, and dashed and dash-dotted curves refer to full CSI case.

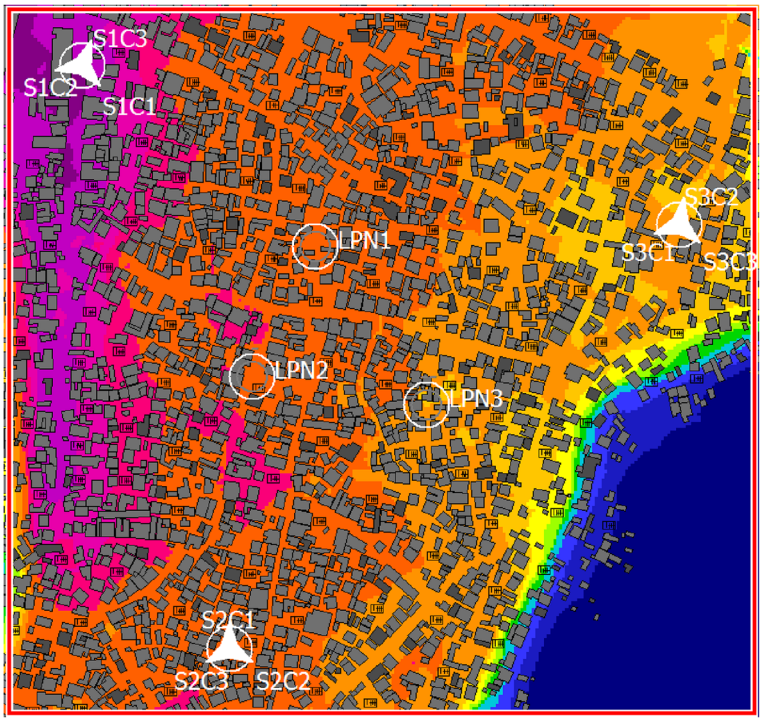

Figure 5 Deployment scenario for the CoMP-enhanced-relay-based HetNet.

2.83-b/s/Hz capacity increments are seen at 50th percentile when $b = 1$ and $b = 3$, respectively. Furthermore, it can be seen that QCP CoMP with a few number of feedback bits (that is, $N_2 = N_3 = 3$) achieves performance close to MRT that assumes full CSI.

4 Simulation case study

Although Section 3 presents analytical expressions to quantify the spectral efficiency gain that can be achieved by applying QCP CoMP at the backhaul of a given LPN, it does not illustrate the trade-off between the CoMP capacity gain and resource scheduling. In this section, we present a stimulation case study that presents the overall throughput gains of CoMP when applied at the backhaul of LTE-Advanced relays deployed in a realistic exemplary deployment scenario.

4.1 Simulation scenario and parameters

The simulation case study focuses on the performance investigation of CoMP-enhanced self-backhauling in a densely populated area. The densely populated area scenario is particularly interesting for low-income underserved urban areas in most emerging markets which will eventually constitute the majority in emerging countries due to rapid urbanization [38]. In these informal settlements, the fixed line-penetration has remained virtually flat over the last few decades [39]. Therefore, mobile network operators in those regions are rapidly upgrading or rolling-out mobile broadband networks, as these provide the only economically feasible means for universal broadband connectivity [39]. In addition to RAT upgrades, operators are obliged to consider network densification with outdoor LPN deployment to meet capacity demands in these fast-expanding urban settlements. However, the low-revenue potential and limited supporting infrastructure means that the cost of operating the LPN (including cost of backhauling the LPNs) has to be minimized and therefore innovative end user-deployed shared-access models should be considered [40].

For the simulation study, we assume that three tri-sector macro eNBs and three cell-edge RNs are deployed in a selected simulation area as illustrated in Figure 5. The label SxCy in Figure 5 is used to refer to cell (or sector) y of tri-sectored macro site x. We note that the LPN in Figure 5 hereafter refers to an LTE-Advanced RN. Furthermore, we deliberately increase the number of macrocell coordination scenarios by placing the 3 RNs at the edges of three adjacent cells, such that each RN is served by a unique cell of a different site from the other two. To be specific using Figure 5, the deployment is such that S1C1 is donor cell for LPN1 (RN1); S2C1 is donor cell for LPN2 (RN2); and S3C1 is donor cell for LPN3 (RN3). The radio coverage estimations behind the deployment are based on realistic three-dimensional (3D) building

vectors and topographical data for a densely settled area (Hanna Nassif in Tanzania) [30]. The radio link loss is evaluated using the dominant path model implemented in the WinProp ray tracing tool [41]. Static system-level simulations are performed to investigate network performance for CoMP and non-CoMP scenarios on the relay link, with UEs being dropped at random locations. In this case, we refer to UEs attached to RNs and macrocells as RUEs and MUEs, respectively. The downlink CoMP simulation parameters and assumptions follow commonly used 3GPP guidelines [22], and key values are listed in Table 1.

4.2 Scheduling and throughput formula

In typical FDD LTE-Advanced type 1 inband relay scenarios, the MUE, RN, and RUE are served on a common frequency band [13]. Time-domain half-duplexing is used to isolate backhaul and access link transmissions, with the RN continuously switching between the relay and access links to avoid self-interference, as illustrated in Figure 6. Note that parameter τ_r denotes time ratio allocated to the backhaul link.

Optimal resource utilization on average is achieved at each RN when τ_r is semi-statically selected by DeNBs such

Table 1 Basic simulation parameters and assumptions

Parameters	Values/assumptions
Air interface	LTE FDD
Carrier frequency/bandwidth	2,110/10 MHz
Simulation	Radio propagation modeling (WinProp) Static sytem level simulation (Matlab) 5-m resolution 1.5-m UE and 5-m RN prediction height
CoMP	Three cooperating cells Downlink JP CoMP QCP with $b = 1$ and $N = 3$ feedback bits
Throughput	$B_{\text{eff}} = 0.62, Z_{\text{eff}} = 1.8, Z_{\text{min}} = -10$ dB, $S_{\text{max}} = 4.4$ b/s/Hz
Macro (DeNB/eNB) parameters	
Macro sites	Site 1 Site 2 Site 3
Transmit power per antenna	46 dBm
Antenna height	18 m 20 m 25 m
Antenna patterns	Kathrein 741984
Sector azimuths	20, 140, 260 0, 120, 240 10, 130, 250
Intersite distance	Approximately 500 m
RN parameters	
Transmit power/antenna gain/noise figure	30 dBm/5 dBi/5 dB
Deployment height	5 m
RN locations	250 m from DeNB, 140 m inter-RN distance
Antenna configuration	1×2
UE (RUE and MUE) parameters	
Noise figure	9 dB
Antenna configuration	1×2
Mean UE number	15 UE per macrocell
UE mobility	Mobility off 50% UEs dropped randomly in whole area 50% UEs cluster-dropped in 40-m radius of RNs
Buildings and fading characteristics	
Buildings	Building of variable dimensions, height 3 to 6 m Building penetration loss: 10 dB
Fading	Shadow fading: dominant path model (WinProp) Fast fading: Rician fading (RN-DeNB, $K = 3$ dB) and Rayleigh fading (other links)

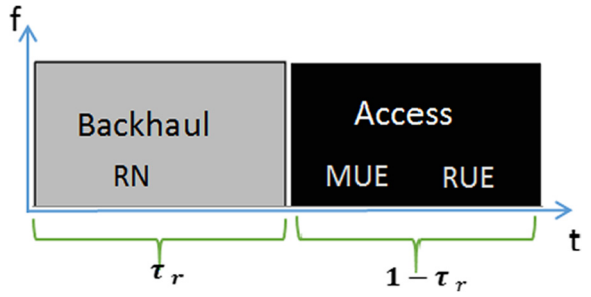

Figure 6 Resource allocation among relay, macro, and relay users.

that $\tau_r \bar{R}_r = (1-\tau_r)\bar{R}_a$, where $\bar{R}_r$ is the average rate at the backhaul and $\bar{R}_a$ is the aggregate rate at the access, both assuming transmission in whole time frame. Accordingly, optimal τ_r and corresponding end-to-end rate can be given as:

$$\hat{\tau}_r = \frac{\bar{R}_a}{(\bar{R}_r + \bar{R}_a)}, \quad \bar{R}_{e2e} = \frac{\bar{R}_r \bar{R}_a}{(\bar{R}_r + \bar{R}_a)} \tag{18}$$

We note here that selection of τ_r semi-statically is attractive as it requires less capacity to feedback long-term feedback information than dynamic selection that requires short-term feedback information although the latter potentially delivers better resource utilization with more overhead. In practice, downlink backhaul radio resources are achieved by allocating RNs up to six multicast-broadcast single frequency network (MBSFN) subframes (frame numbers 0, 1, 2, 3, 6, 7, 8) out of the ten subframes (each of 1 ms duration) specified in the 3GPP Release 8 LTE frame structure [42]. Thus, τ_r can take granular values such that $\tau_r \in \{0.1, 0.2, 0.3, 0.4, 0.5, 0.6\}$.

We have three ranges to which values of $\hat{\tau}_r$, computed according to Equation 18, can lie: $\hat{\tau}_r > 0.6$, $0.1 < \hat{\tau}_r < 0.6$, and $\hat{\tau}_r < 0.1$. If $\hat{\tau}_r > 0.6$, then backhaul is a bottleneck. If $0.1 < \hat{\tau}_r < 0.6$, then we can balance the backhaul and access. Moreover, $\hat{\tau}_r < 0.1$ means access is a bottleneck. In conventional relay deployment scenarios including this case study, the former is the most likely case. Therefore, we select values of τ_r statically in our simulation. Note here that the higher values of selected τ_r, the better the backhaul capacity but the worst MUE (allocated $1-\tau_r$ fraction of time resources) throughput. We will revise the discussion on τ_r selection and performance trade-off in Subsection 4.3 based on the simulation results.

In the relay access, the RN performs scheduling decision in each subframe or transmission time interval (TTI), whereby, RUEs are allocated a fraction of the total physical resource blocks (PRBs) available in the subframe. It should be noted that no RUEs are scheduled during the backhaul subframes when the RN will have reverted to relay link operation in the half-duplex configuration. The actual scheduler implementation (round robin (RR), proportional fair, etc.) for RN access resources is vendor specific as in the case of eNBs [42]. We initially apply here RR scheduling to divide the resources equally among RUEs so that we can observe throughput gap between backhaul and access. In the case that the backhaul presents a capacity bottleneck ($R_r < R_a$), the initially allocated resources using RR scheduling are redistributed among the RUEs using max-min fair scheduling which priorities RUEs with lower throughputs [43]. Otherwise, if backhaul is not a bottleneck ($R_r \geq R_a$), the resource allocation for the RUEs from RR scheduling is retained.

During coordination among cells in CoMP set for joint relay link transmissions in each backhaul subframe, orthogonal frequency resource allocation is applied among the set of served RNs. We apply here basic RR resource partitioning strategy where relay link resources (subcarriers) are partitioned equally among relay link transmissions. Note that advanced CSI-based scheduling methods, such as proportional fair, can be applied to achieve better performance.

Throughput (TP) in both the backhaul and access links is computed through mapping SINRs results using a modified Shannon formula [44]:

$$\mathrm{TP} = \tau N_{\mathrm{PRB}} B_{\mathrm{PRB}} * \begin{cases} \min\{B_{\mathrm{eff}} \log_2\left(1 + \frac{Z}{Z_{\mathrm{eff}}}\right), S_{max}\}, & Z \geq Z_{\min} \\ 0, & Z < Z_{\min}, \end{cases} \tag{19}$$

where τ reflects the amount of time resource allocated for the transmission, N_{PRB} is the number of PRBs, and B_{PRB} is the bandwidth per PRB. Note also that $S_{\max}$ is the maximum spectral efficiency, $Z_{\min}$ is the minimum required SINR, B_{eff} adjusts the system bandwidth efficiency to fit with LTE, and Z_{eff} adjusts for the SINR implementation efficiency. We recall that $\tau = \tau_r$ for backhaul links and $\tau = 1 - \tau_r$ for access links. Parameters B_{eff}, Z_{eff}, $S_{\max}$, and $Z_{\min}$ are obtained from link-level simulations and curve fitting. We consider a 1×2 MIMO configuration for the simulation and values of the parameters computed for the configuration are listed in Table 1 [45].

4.3 Simulation results and performance evaluation

The CDF of the backhaul and access throughput considering all relays is illustrated in Figure 7. The value of τ_r is set to the maximum 0.6 for both CoMP and non-CoMP cases.

We can clearly see from Figure 7 that QCP-CoMP significantly improves the backhaul throughput (end-to-end throughput) and diminishes the gap between the backhaul and access. It reduces the 219.12%, 112.43%, and 52.62% relative throughput gap for no-CoMP case at 10-ile, 50%-ile and 90%-ile to 5.67%, 8.00%, and 22.81% relative throughput gap, respectively.

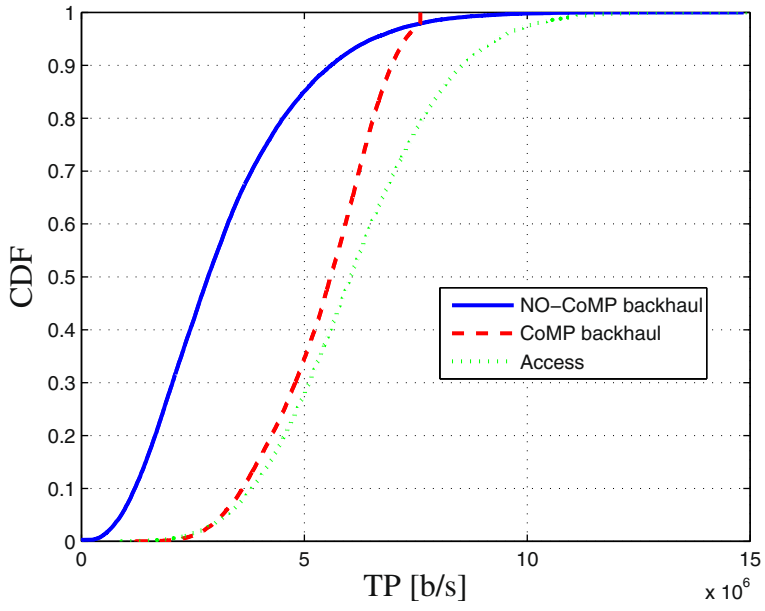

Figure 7 Cumulative distribution function of backhaul and access throughput. Solid curve refers to results for non-CoMP backhaul whereas dashed and dotted curves refer to results for CoMP backhaul and access, respectively.

We illustrate contribution of CoMP-enhanced backhaul on the RUE throughput using a bar plot depicted in Figure 8. The plot shows CoMP gains over non-CoMP scenario when $\tau_r = 0.6$ and $\tau_r = 0.3$. We see that the applied CoMP scheme for both $\tau_r = 0.6$ and $\tau_r = 0.3$ significantly improves all the 10%-ile, 50%-ile, and 90%-ile RUE throughputs. Unlike $\tau_r = 0.6$ case, the scheme helps more the 10%-ile and 50%-ile when $\tau_r = 0.3$. Furthermore, the plot in Figure 8 shows throughput gains of CoMP when $\tau_r = 0.3$ over non-CoMP case when $\tau_r = 0.6$. We see that there are still gains at 10%-ile and 50%-ile although loss is experienced at 90%-ile. Note that the reduction in τ_r allows for more time resources to be allocated for MUEs thus enhancing MUE throughput performance.

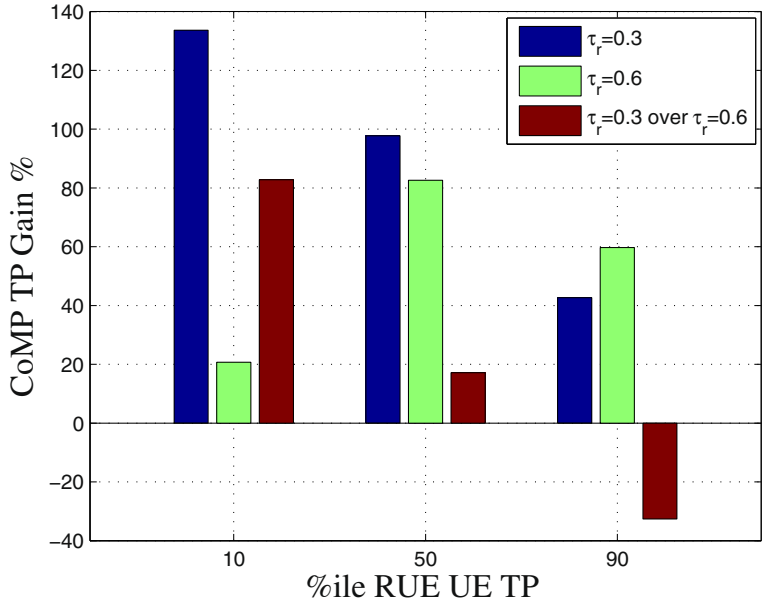

Figure 8 CoMP gain in terms of RUE 10%-ile, 50%-ile, and 90%-ile throughput when $\tau_r = 0.6$ and $\tau_r = 0.3$.

Performance impact of the CoMP technique in all UEs (both RUEs and MUEs) is illustrated in Figure 9. We see that CoMP delivers 10%-ile, 50%-ile, and 90%-ile percentage gains of 85.96%, 56.98%, and 0.15% when $\tau_r = 0.3$, respectively. The percentage gain values are 8.48%, 43.83%, and 33.59% when $\tau_r = 0.6$. Note that CoMP improvements are more for the lower percentile throughput when $\tau_r = 0.3$ unlike the case when $\tau_r = 0.6$ where improvements are more for the higher percentile throughputs. If we compare CoMP with $\tau_r = 0.3$ and non-CoMP with $\tau_r = 0.6$, we see that CoMP with $\tau_r = 0.3$ provides 81.89%, 26.38%, and 24.07% gains at 10%-ile, 50%-ile, and 90%-ile, respectively, relative to the case of non-CoMP with $\tau_r = 0.6$.

In order to show the impact of CoMP on the consistency of UE throughput experience, we also present in Figure 10 the CDF of fairness index defined as [46]:

$$\mathrm{FI} = \frac{\left[\sum_{i=1}^{N_{\mathrm{ue}}} \mathrm{TP}_i\right]^2}{N_{\mathrm{ue}} \sum_{i=1}^{N_{\mathrm{ue}}} \mathrm{TP}_i^2}, \tag{20}$$

where N_{ue} is total number of UEs. The figure clearly shows that CoMP provides more consistent user experiences for both $\tau_r = 0.3$ and $\tau_r = 0.6$.

4.4 Performance evaluation under feedback error

Figure 11 depicts the CDF of the backhaul throughput considering errors in CoMP phase feedback bits when $\tau_r = 0.6$. The throughput CDF of the non-COMP case is presented as a benchmark considering a similar value $\tau_r = 0.6$. Solid curve refers to results for non-CoMP backhaul while dashed, dotted, and dash-dotted curves refer to results for CoMP backhaul under 0%, 10%, and 20% bit error probability, respectively. We assume 3-bit Gray coding and uniformly distributed errors in the simulation. We observe from Figure 11 that large feedback bit-error probability can considerably diminish the CoMP benefit of narrowing the capacity gap between backhaul and access. For instance, the 92.19% gap reduction obtained at 10%-ile in the absence of feedback error is reduced to 72.42% and 51.64% for 10% and 20% feedback bit-error probability, respectively. As a result, the feedback error negatively impacts the CoMP throughput gain of RUEs as illustrated in Figure 12. The gain reduction at 10%-ile RUE throughput due to feedback bit error is considerably higher when $\tau_r = 0.3$. On the other hand, the reduction due to feedback error when $\tau_r = 0.3$ and $\tau_r = 0.6$ is almost the same at 50%-ile.

5 Conclusions

In this paper, we discussed some of the key operator considerations in the selection of LPN backhauling solutions. The use of self-backhauling for LPNs by exploiting the existing macro RAN was highlighted as a promising method both in terms of cost-effectiveness of backhaul implementation and flexibility of LPN deployment. The backhaul capacity bottleneck which limits the LPN capacity was underlined as the primary limitation for the self-backhauling approach. To that end, we investigated the use of CoMP transmission for relaxing the downlink backhaul capacity bottleneck for self-backhauled LPNs. We approached this work from two

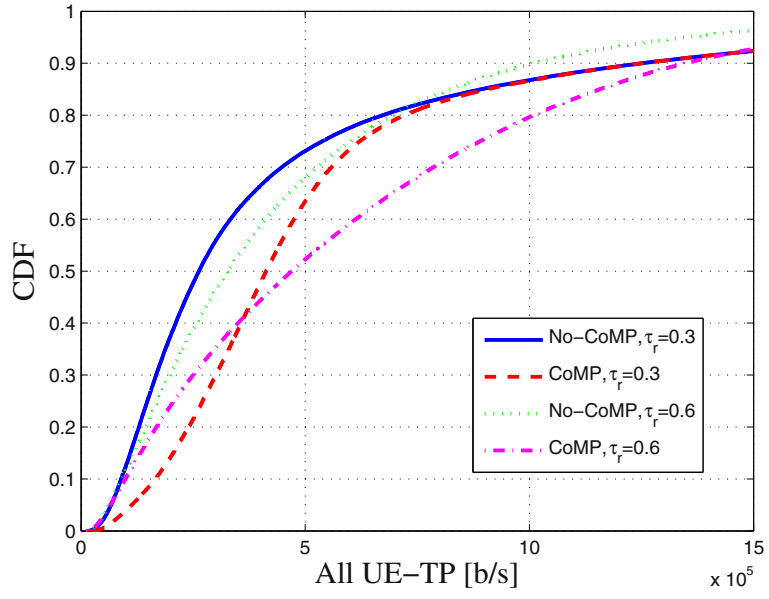

Figure 9 Cumulative distribution function of all UE throughput. Solid and dashed curves refer to results for non-CoMP and CoMP cases, respectively, when $\tau_r = 0.3$ whereas dotted and dash-dotted curves refer to non-CoMP and CoMP cases, respectively, when $\tau_r = 0.6$.

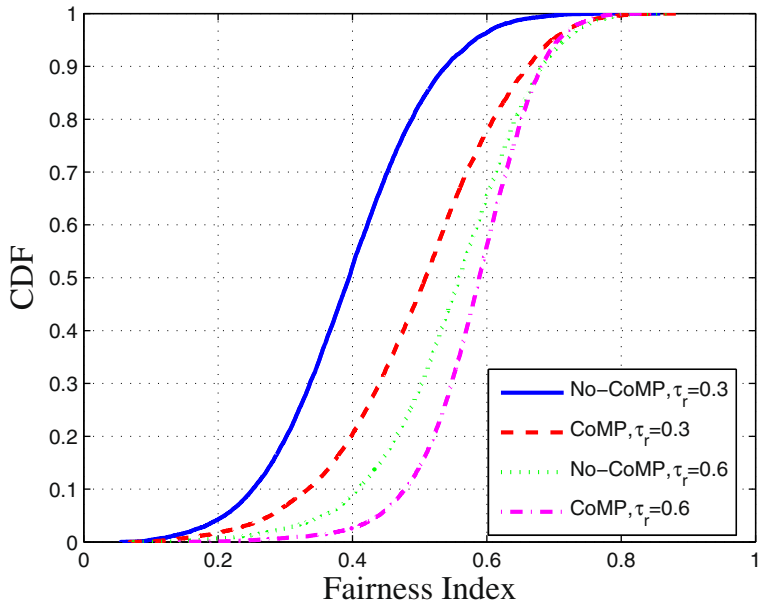

Figure 10 Cumulative distribution function of fairness index. Solid and dashed curves refer to results for non-CoMP and CoMP cases, respectively, when $\tau_r = 0.3$ whereas dotted and dash-dotted curves refer to results for non-CoMP and CoMP cases, respectively, when $\tau_r = 0.6$.

ways. First, an analytical study was conducted to find analytical expression for capacity outage probability for a practical limited-feedback CoMP technique. In this context, CoMP was considered for relaxing backhaul capacity bottlenecks in general self-backhauled LPNs. Secondly, we carried out an extensive simulation campaign for an exemplary HetNet deployment in a realistic dense settlement scenario, whereby the aforementioned CoMP technique was used for relaxing downlink backhaul capacity bottlenecks for LTE-Advanced type 1 relays.

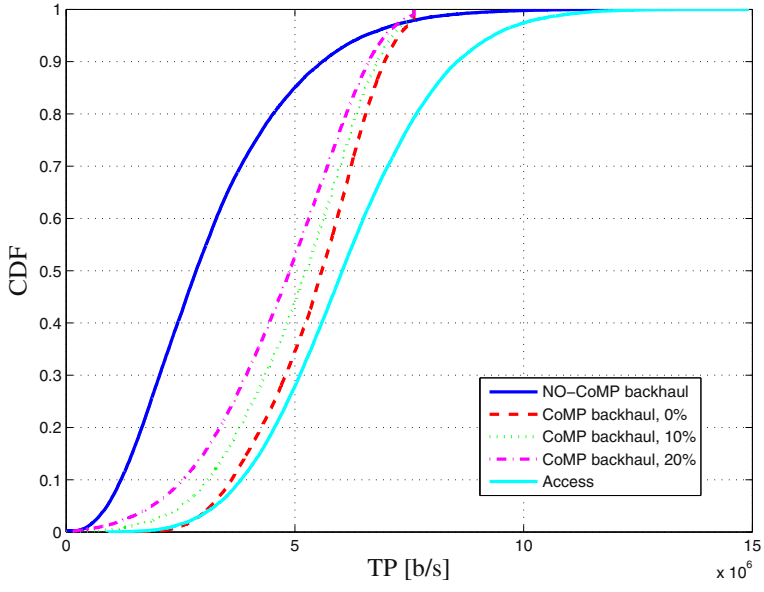

Figure 11 Cumulative distribution function of backhaul and access throughput under feedback bit error. Solid curves refers to results for non-CoMP backhaul and access, whereas dashed, dotted, and dash-dotted curves refer to results for CoMP backhaul assuming 0%, 10%, and 20% bit error probability, respectively, when $\tau_r = 0.6$.

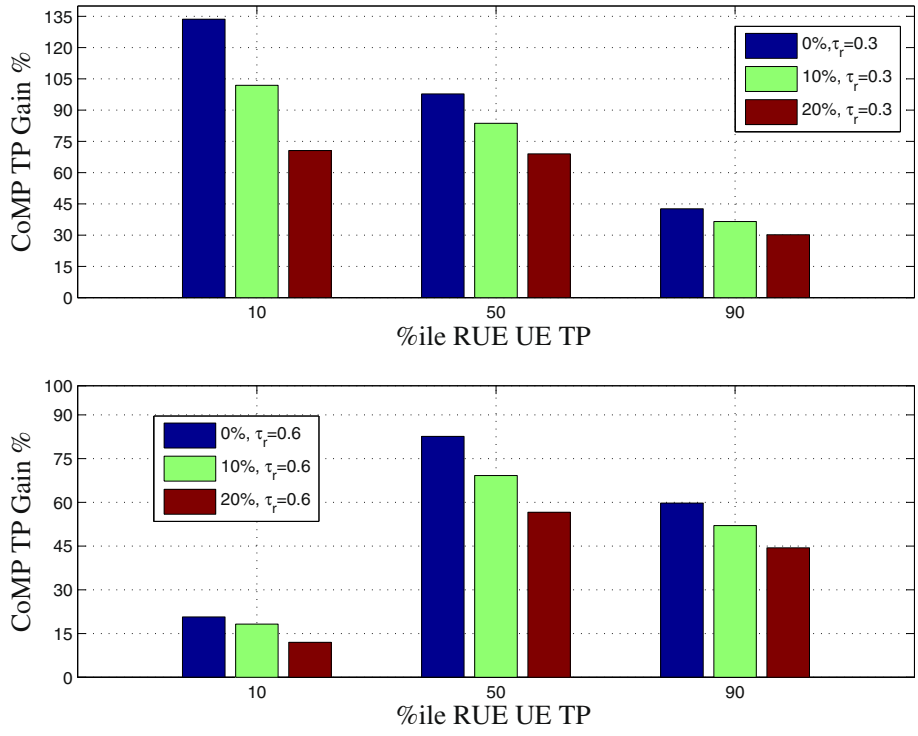

Figure 12 CoMP gain in terms of RUE 10%-ile, 50%-ile, and 90%-ile throughput. For 0%, 10% and 20% bit error probability cases when $\tau_r = 0.6$ and $\tau_r = 0.3$.

Analytical results show that we can considerably increase expected capacity for a certain outage probability by the CoMP method. For instance, a capacity increase by 4.37 b/s/Hz was noted at the 50%-ile when each cell in the CoMP set transmits with full power, and the LPN applies a feedback word of 3 bits for each cell in the CoMP set (except for the donor cell). Furthermore, the CoMP method performs close to the ideal maximum ratio transmission even with the 3-bit feedback word.

Throughput results obtained from the simulation campaign assert that the CoMP scheme significantly improves the capacity gap between backhaul and access. For instance, the gap is reduced by 86.00% at the 50%-ile when we allocate 60% of the LTE subframes for the backhaul. The enhancement is accompanied by an approximately 80% RUE throughput gain at 50%-ile. When 30% of the subframes are allocated for the backhaul, we note a relatively higher RUE throughput gain at the 10%-ile and 50%-ile (compared to the case with 60% of subframes allocated for the backhaul). Besides, we can use the CoMP gain at the backhaul to increase the percentage of subframes for MUE (decrease subframes for backhaul) so that throughput is improved not only for RUEs but also for MUEs. We observe that CoMP with 30% backhaul subframes provides 26.38% throughput gain for all UEs at 50%-ile relative to the case of non-CoMP with 60% backhaul subframes. Furthermore, the fairness index shows that the use of CoMP for LPN backhaul provides more even throughput distribution among UEs in both 60% and 30% subframe configurations for the backhaul. Although these CoMP performance gains are sustained under feedback error, it was also noted that considerable reduction in the gains are observed for large bit-error probability ($\geq$ 10%) .

Possible future work includes computation of analytical expressions for multi-antenna scenarios and performance measures (such as average capacity) that were not considered herein, and comparative analysis of various CoMP techniques with different requirements (amount of overhead, shared information, implementation requirements, and so on). Also of interest would be the consideration of various clustering methods (static, dynamic, or hybrid) to define the CoMP set. Furthermore, we could consider semi-static resource allocation (backhaul subframe selection) to balance backhaul and access capacity. The overall research question that needs to be addressed is how to use CoMP efficiently and adaptively for the right LPN and at the right moment.

Competing interests

The authors declare that they have no competing interests.

Acknowledgements

This work was performed within the ICT&E project funded by the Aalto University School of Electrical Engineering programme on energy efficiency

and EWINE-S project, funded in part by the Finnish Funding Agency for Technology and Innovation, European Communications Engineering and Efore Oyj. Hanna Nassif GIS data was kindly provided by Prof. R. Sliuzas of the ITC-Faculty of Geo-Information Science and Earth Observation, University of Twente.

Received: 7 August 2014 Accepted: 9 February 2015
Published online: 20 March 2015

References

1. J Zander, Mahonen P, Riding the data tsunami in the cloud: myths and challenges in future wireless access. IEEE Commun. Mag. **51**(3), 145–151 (2013)
2. Small Cell Forum. Small cells - what is the big idea? TR Doc. 030.01.01, SCF Release 1 (February 2012). http://smallcellforum.org/smallcellforum/Files/File/SCF-Small_Cells_White_Paper.pdf. Accessed 03 March 2015
3. I Hwang, B Song, SS Soliman, A holistic view on hyper-dense heterogeneous and small cell networks. IEEE Commun. Mag. **51**(6), 20–27 (2013)
4. JG Andrews, H Claussen, M Dohler, S Rangan, MC Reed, Femtocells: Past, present, and future. IEEE J. Sel. Areas Commun. **30**(3), 497–508 (2012)
5. Andrews JG, Seven ways that HetNets are a cellular paradigm shift. IEEE Commun. Mag. **51**(3), 136–144 (2013)
6. J Robson, Small cell deployment strategies and best practice backhaul. white paper, Cambridge broadband networks, (August 2012). http://cbnl.com/resources/small-cell-strategies. Accessed 03 Macrch 2015
7. NGMN, Small cell backhaul requirements. white paper, NGMN Alliance, (June 2012). http://www.ngmn.org/uploads/media/NGMN_Whitepaper_Small_Cell_Backhaul_Requirements.pdf. Accessed 03 March 2015
8. NSN, Outdoor 3G/LTE small cells deployment strategy: 'the race to the pole'. white paper (2013). http://networks.nokia.com/sites/default/files/document/nokia_outdoor_3glte_small_cells_deployment_strategy_whitepaper.pdf. Accessed 03 March 2015
9. FP7 METIS, Scenarios, requirements and KPIs for 5G mobile and wireless system. Project deliverable d1.1 (April 2014). https://www.metis2020.com/wp-content/uploads/deliverables/METIS_D1.1_v1.pdf. Accessed 03 March 2015
10. Flyyn K, Delivering public safety communications with LTE, 3gpp news (July 2013). http://www.3gpp.org/news-events/3gpp-news/1455-Public-Safety
11. T Sakano, ZM Fadlullah, T Ngo, H Nishiyama, M Nakazawa, F Adachi, N Kato, A Takahara, T Kumagai, H Kasahara, Kurihara S, Disaster-resilient networking: a new vision based on movable and deployable resource units. IEEE Netw. **27**(4), 40–46 (2013)
12. P Blasco, M Bennis, M Dohler, in *Paper presented at the 2013 IEEE international conference on communications*. Backhaul-aware self-organizing operator-shared small cell networks (IEEE, Budapest, 9–13 June 2013)
13. C Hoymann, W Chen, J Montojo, A Golitschek, C Koutsimanis, X Shen, Relaying operation in 3GPP LTE: challenges and solutions. IEEE Commun. Mag. **50**(2), 156–162 (2012)
14. Qualcomm, Rising to meet the 1000x mobile data challenge. white paper (2012). http://www.qualcomm.com/media/documents/
15. Z Roth, M Goldhamer, N Chayat, A Burr, M Dohler, N Bartzoudis, C Walker, Y Leibe, C Oestges, M Brzozowy, I Bucaille, in *Paper presented at the 2010 future network and mobile summit*. Vision and architecture supporting wireless GBit/sec/km^2 capacity density deployments (IEEE, Florence, 16-18 June 2010)
16. IEEE, Architecture and requirements for small cell backhaul (2013). Technical report, IEEE 802.16r
17. O Bulakci, S Redana, B Raaf, J Hamalainen, in *Paper presented at the 2010 71st vehicular technology conference (VTC 2010-Spring)*. Performance enhancement in LTE-Advanced relay networks via relay site planning (IEEE, Taipei, 16–19 May 2010)
18. O Bulakci, A Bou Saleh, J Hamalainen, S Redana, Performance analysis of relay site planning over composite fading/shadowing channels with cochannel interference. IEEE Trans. Veh. Technol. **62**(4), 1692–1706 (2013). doi:10.1109/TVT.2012.2233506
19. A Saleh, O Bulakci, J Haḿaḿlaḷinen, S Redana, B Raaf, Analysis of the impact of site planning on the performance of relay deployments. IEEE Trans. Veh. Technol. **61**(7), 3139–3150 (2012). doi:10.1109/TVT.2012.2202253
20. I Marić, B Boštjančič, A Goldsmith, in *Paper presented at the 2011 information theory and applications workshop (ITA)*. Resource allocation for constrained backhaul in picocell networks (IEEE, 6–11 February 2011)
21. M Sawahashi, Y Kishiyama, A Morimoto, D Nishikawa, M Tanno, Coordinated multipoint transmission/reception techniques for LTE-Advanced. IEEE Wireless Commun. Mag. **17**(3), 26–34 (2010). doi:10.1109/MWC.2010.5490976
22. 3GPP: Coordinated multi-point operation for LTE physical layer aspects. TR 36.819, Ver. 11.0.0, 3GPP Technical Report (2011). http://www.3gpp.org/dynareport/36819.htm. Accessed 03 March 2015
23. V Garcia, N Lebedev, J-M Gorce, Capacity outage probability for multi-cell processing under Rayleigh fading. Commun. Lett. IEEE. **15**(8), 801–803 (2011)
24. B Luo, Q Cui, X Tao, D Alexis, in *Paper presented at the 2013 IEEE international conference on communications*. On the optimal power allocation for coordinated wireless backhaul in OFDM-based relay systems (IEEE, Budapest, 9–13 June 2013)
25. DJ Love, RW Heath, VKN Lau, D Gesbert, BD Rao, M Andrews, An overview of limited feedback in wireless communication systems. IEEE J. Sel. Areas Commun. **26**(8), 1341–1365 (2008)
26. S Sun, Q Gao, Y Peng, Y Wang, L Song, Interference management through CoMP in 3GPP LTE-advanced networks. IEEE Trans. Wireless Commun. **20**(1), 59–66 (2013)
27. J Zhao, TQS Quek, Z Lei, Coordinated multipoint transmission with limited backhaul data transfer. IEEE Trans. Wireless Commun. **12**(6), 2762–2775 (2013)
28. R Irmer, H Droste, P Marsch, M Grieger, G Fettweis, S Brueck, H-P Mayer, L Thiele, V Jungnickel, Coordinated multipoint: concepts, performance, and field trial results. IEEE Commun Mag. **29**, 102–111 (2011). doi:10.1109/MCOM.2011.5706317
29. J Hämäläinen, Wichman R, in *Proc. Asilomar Conf. on Signals, Systems and Computers*, vol. 1. Closed-loop transmit diversity for FDD WCDMA systems, (2000), pp. 111–115. doi:10.1109/ACSSC.2000.910927
30. BB Haile, E Mutafungwa, J Hamalainen, in *Paper presented at the 2013 AFRICON*. Coordinated multipoint transmission for LTE-Advanced networks in dense informal settlements (IEEE Pointe-Aux-Piments, 9–12 September 2013)
31. A Narula, MJ Lopez, MD Trott, GW Wornell, Efficient use of side information in multiple-antenna data transmission over fading channels. IEEE J. Sel. Areas Commun. **16**(8), 1423–1436 (1998). doi:10.1109/49.730451
32. 3GPP, Physical layer procedures (FDD). TS 25.214, Ver. 10.4.0, 3GPP Technical Specification (2011). http://www.3gpp.org/DynaReport/25214.htm. Accessed 03 March 2015
33. 3GPP, Physical channels and modulation (2011). TS 36.211, Ver. 10.3.0, 3GPP Technical Specification
34. Y-D Yao, AUH Sheikh, Outage probability analysis for microcell mobile radio systems with cochannel interferers in Rician/Rayleigh fading environment. Electron. Lett. **26**(13), 864–866 (1990)
35. SM Ross, *Introduction to Probability Models*. (Academic Press, San Diego, 2000)
36. AA Dowhuszko, G Corral-Briones, J Hämäläinen, Wichman R, On throughput-fairness tradeoff in virtual MIMO systems with limited feedback. EURASIP J. Wireless Commun. Netw. **2009**, 1–17 (2009). doi:10.1155/2009/102064
37. M Abramowitz, IA Stegun, *Handbook of Mathematical Functions with Formulas, Graphs, and Mathematical Tables*, Ninth dover printing, tenth gpo printing. (Dover, New York, 1964)
38. UN-HABITAT, Slum dwellers to double by 2030. report (April 2007). http://www.un.org/apps/news/story.asp?newsid=8427&cr=&cr1=. Accessed 03 March 2015
39. GSMA, Sub-Saharan Africa Mobile Observatory 2012. report November 2012. http://www.gsma.com/publicpolicy/wp-content/uploads/2012/03/SSA_FullReport_v6.1_clean.pdf. Accessed 03 March 2015
40. P Amin, NS Kibret, E Mutafungwa, BB Haile, J Hamalainen, JK Nurminen, in *Paper presented at the 25th IEEE international symposium on personal, indoor and mobile radio communications (PIMRC)*. Performance study for off-grid self-backhauled small cells in dense informal settlements (IEEE, Washington DC, 2–5 September 2014)

41. WinProp Software Package. http://www.awe-communications.com/
42. H Holma, A Toskala, *LTE for UMTS - OFDMA and SC-FDMA Based Radio Access*. (Wiley, Chichester, 2009)
43. A Coluccia, D A'Alconzo, F Ricciato, On the optimality of max-min fairness in resource allocation. Ann. Telecommun. **67**(1–2), 15–26 (2012)
44. P Mogensen, W Na, IZ Kovacs, F Frederiksen, A Pokhariyal, KI Pedersen, T Kolding, K Hugl, M Kuusela, in *Paper presented at the IEEE 2007, 65th vehicular technology conference*. LTE capacity compared to the Shannon bound (IEEE, Dublin, 22–25 April 2007)
45. E Lahetkangas, K Pajukoski, E Tiirola, J Hamalainen, Z Zheng, in *Poznan*. On the performance of LTE-Advanced MIMO: How to set and reach beyond 4G targets (Poland, 18–20 April 2012)
46. R Jain, D Chiu, W Hawe, A quantitative measure of fairness and discrimintation for resource allocation in shared computer systems. TR 301, Digital Equipment Corporation Technical Report September 1984. http://www.cs.wustl.edu/~jain/papers/ftp/fairness.pdf. Accessed 03 March 2015